

# UC Davis

## UC Davis Previously Published Works

### Title

Effects of carnitine palmitoyltransferases on cancer cellular senescence

### Permalink

<https://escholarship.org/uc/item/92z5d060>

### Journal

Journal of Cellular Physiology, 234(2)

### ISSN

0021-9541

### Authors

Guan, Lihuan  
Chen, Yixin  
Wang, Yongtao  
et al.

### Publication Date

2019-02-01


### DOI

10.1002/jcp.27042

Peer reviewed

## ORIGINAL RESEARCH ARTICLE

# Effects of carnitine palmitoyltransferases on cancer cellular senescence

Lihuan Guan<sup>1</sup> | Yixin Chen<sup>1</sup> | Yongtao Wang<sup>1</sup> | Huizhen Zhang<sup>1</sup> | Shicheng Fan<sup>1</sup> | Yue Gao<sup>1</sup> | Tingying Jiao<sup>1</sup> | Kaili Fu<sup>1</sup> | Jiahong Sun<sup>1</sup> | Aiming Yu<sup>2</sup> | Min Huang<sup>1</sup> | Huichang Bi<sup>1</sup> 

<sup>1</sup>Institute of Clinical Pharmacology and Guangdong Provincial Key Laboratory of New Drug Design and Evaluation, School of Pharmaceutical Sciences, Sun Yat-sen University, Guangzhou, China

<sup>2</sup>Department of Biochemistry & Molecular Medicine, Comprehensive Cancer Center, UC Davis School of Medicine, Sacramento, California

**Correspondence**

Huichang Bi, PhD, School of Pharmaceutical Sciences, Sun Yat-sen University, 132# Waihuandong Road, Guangzhou University City, Guangzhou 510006, China.  
Email: bihchang@mail.sysu.edu.cn

**Funding information**

National Natural Science Foundation of China, Grant/Award Numbers: 81522047, 81573489, 81320108027; National Key Research and Development Program, Grant/Award Numbers: 2017YFE0109900, 2017YFC0909303; 111 project, Grant/Award Number: B16047; Key Laboratory Foundation of Guangdong Province, Grant/Award Number: 2017B030314030; Natural Science Foundation of Guangdong, Grant/Award Numbers: 2017A030311018, 2015A030313124

The carnitine palmitoyltransferase (CPT) family is essential for fatty acid oxidation. Recently, we found that CPT1C, one of the CPT1 isoforms, plays a vital role in cancer cellular senescence. However, it is unclear whether other isoforms (CPT1A, CPT1B, and CPT2) have the same effect on cellular senescence. This study illustrates the different effects of CPT knockdown on PANC-1 cell proliferation and senescence and MDA-MB-231 cell proliferation and senescence, as demonstrated by cell cycle kinetics, Bromodeoxyuridine incorporation, senescence-associated  $\beta$ -galactosidase activity, colony formation, and messenger RNA (mRNA) expression of key senescence-associated secretory phenotype factors. CPT1C exhibits the most substantial effect on cell senescence. Lipidomics analysis was performed to further reveal that the knockdown of CPTs changed the contents of lipids involved in mitochondrial function, and lipid accumulation was induced. Moreover, the different effects of the isoform deficiencies on mitochondrial function were measured and compared by the level of radical oxygen species, mitochondrial transmembrane potential, and the respiratory capacity, and the expression of the genes involved in mitochondrial function were determined at the mRNA level. In summary, CPT1C exerts the most significant effect on mitochondrial dysfunction-associated tumor cellular senescence among the members of the CPT family, which further supports the crucial role of CPT1C in cellular senescence and suggests that inhibition of CPT1C may represent as a new strategy for cancer treatment through the induction of tumor senescence.

**KEYWORDS**

carnitine palmitoyltransferase (CPT), cellular senescence, lipidomics, mitochondrial function

## 1 | INTRODUCTION

Cellular senescence, a heterogeneous and complicated process, is broadly defined as a state of stable exit from the cell cycle (Pérez-Mancera, Young, & Narita, 2014). Cellular senescence can be triggered in response to multiple factors, such as oncogene deregulation, oxidative stress, mitochondrial dysfunction, and

genomic instability (Campisi & D'Adda, 2007; Gallage & Gil, 2016). During senescence, cells develop a distinctive phenotype, typified by changes in morphology, activation of  $\beta$ -galactosidase, absence of proliferative markers, expression of tumor suppressors and cell cycle inhibitors, secretion of pro-inflammatory signaling molecules and so on (Muñoz-Espín & Serrano, 2014). Mounting evidence has shown that the senescence response is recognized as one of the formidable

barriers to malignant tumorigenesis (Campisi, 2005). To suppress the development of cancer, it is important to examine drivers of senescence.

The carnitine palmitoyltransferase (CPT) system consists of two distinct proteins located in the outer (CPT1) and inner (CPT2) mitochondrial membranes (Bonfont et al., 1999). CPT1 has three tissue-specific isoforms. CPT1A is found in liver, CPT1B in muscle, and CPT1C is mainly expressed in the brain and testes, while CPT2 is ubiquitously expressed (Britton et al., 1995; Demaugre et al., 1991; Price et al., 2002; Yamazaki et al., 1996). CPT constitutes an important element for the regulation of fatty acid oxidation (FAO) and maintenance of energy homeostasis. CPT1A and CPT1B catalyze carnitine and acyl-CoA to form acylcarnitine, and CPT2 reverses the reaction to form acyl-CoA, which results in the transportation of fatty acids from the cytosol into the mitochondria for  $\beta$ -oxidation, especially long chain fatty acids (LCFAs; Bonfont, 2004). CPT1A has been reported to be associated with cancer cell proliferation and metastasis via altering FAO (Pacilli et al., 2013). The intervention on CPT1A expression could be a potential molecular therapy for obesity and diabetes by enhancing hepatic FAO, which is also involved in the treatment of nonalcoholic fatty liver disease (Orellana-Gavaldà et al., 2011; Stefanovic-Racic et al., 2008). A latest finding shows that lower expression of CPT1B inhibits breast cancer stem cell survival (Wang et al., 2017). Other studies on CPT1B are mainly related to the regulation of rapid eye movement sleep and body weight (Cingoz et al., 2014; Ka et al., 2013). Moreover, CPT1B is important to hibernators for energy metabolism due to its higher protein expression in brown fat during hibernation (Eddy, Morin, & Storey, 2006). Although the brain-specific CPT1C is structurally similar to its paralogs CPT1A and CPT1B, it exhibits much lower catalytic activity (Gratacós et al., 2008). In fact, it is documented that CPT1C plays a pivotal role in the regulation of energy homeostasis, food intake, and ceramide metabolism (Carrasco et al., 2012; Wolfgang & Lane, 2011; Wolfgang et al., 2006). Furthermore, the existing evidence suggests that CPT1C is highly expressed in various types of tumors based on the examination of messenger RNA (mRNA) levels (Reilly & Mak, 2012). For CPT2, accumulating reports showed that CPT2 deficiency can lead to several clinical presentations that are individualized according to tissue distribution of the symptoms and the age of onset (Bonfont, 2004).

Recently, we found that CPT1C plays a major role in the regulation of cancer cell senescence through mitochondria-associated metabolic reprogramming, and CPT1C has been shown to be a novel biomarker and a key regulator of cancer cell senescence (Wang et al., 2018). However, it is unclear whether other isoforms (CPT1A, CPT1B, and CPT2) have the same effects on cellular senescence. Thus, this study aimed to compare the effects of CPT knockdown on tumor cellular senescence by evaluating their effects on cell proliferation ability, lipid change, mitochondrial function, and proliferation-related gene expression. The results showed that CPT1C exerts the most significant effect on mitochondrial dysfunction-associated tumor cellular senescence among the members of the CPT family, which further supports CPT1C as a novel target for the intervention on cellular senescence and suggests a new strategy for cancer treatment through induction of tumor senescence.

## 2 | MATERIALS AND METHODS

### 2.1 | Cell culture

The human pancreas cancer cell line PANC-1 was purchased by Guangzhou Cellcook Biotech Company (Guangzhou, China), and the breast cancer cell line MDA-MB-231 was generously provided by Dr. Jun Du at Sun Yat-sen University. Cells were cultured in Dulbecco modified Eagle medium (Corning, NY) containing 4.5 g/L glucose, L-glutamine and sodium pyruvate supplemented with 10% fetal bovine serum, 100 U/ml penicillin sodium, and 100  $\mu$ g/ml streptomycin sulfate (Gibco, NY) in a humidified incubator at 5% CO<sub>2</sub> and 37°C. PANC-1 and MDA-MB-231 were authenticated by authorizing Guangzhou Cellcook Biotech Company utilizing Short Tandem Repeat Authentication.

### 2.2 | Transfection with small interfering RNA

For RNA interfering experiments, small interfering RNAs (siRNA) (Ruibo Biotech Company, Guangzhou, China) were transfected to decrease the CPT1A, CPT1B, CPT1C, CPT2 levels in PANC-1 cells and MDA-MB-231 cells. Quantified cells were seeded and transfected with 50 nM siRNA using Lipofectamine RNAiMAX Transfection Reagent (Invitrogen Life Sciences, CA) with Opti-MEM (Gibco) according to the manufacturer's protocol. The sequence of CPT siRNAs is presented in Supporting Information Table S1. RT-PCR and western blot were performed to measure the mRNA and protein level of CPTs, respectively, to validate the transfection efficiency of three different siRNA chains of CPTs in PANC-1 and MDA-MB-231 cell lines. Then, the most effective ones were chosen to carry out other experiments.

### 2.3 | Quantitative real-time PCR analysis

Total RNA was extracted from cultured cells using Trizol reagent (Invitrogen Life Sciences). The quality and quantity of RNA were examined by a NanoDrop Flex Station 3 spectrophotometer (Thermo Fisher Scientific, CA). Single-strand complementary DNA was synthesized from randomly reverse transcription of about 1  $\mu$ g purified RNA using a Primer Script RT reagent Kit with a gDNA eraser (TaKaRa Biotech, Kyoto, Japan). qRT-PCR was performed using SYBR Premix Ex Taq II kit (TaKaRa Biotech) in 7500 Real-Time PCR System (Applied Biosystems, CA). The fold changes were calculated according to the  $2^{-\Delta\Delta C_t}$  method. The sequences of specific primers are listed in Supporting Information Table S2.

### 2.4 | Western blot analysis

Cells were washed twice with cold phosphate buffer saline (PBS) (Gibco) and lysed by using radioimmunoprecipitation assay lysis buffer containing 1% 100 mM phenylmethylsulfonyl fluoride to prepare total protein, which was then quantified by a BCA protein assay kit (Thermo Fisher Scientific). Total protein was separated by sodium dodecyl sulfate-polyacrylamide gel electrophoresis. Blots were incubated overnight at 4°C with different antibodies against GAPDH

(Santa Cruz Biotechnology, CA), CPT1A, CPT1C, and CPT2 (Abcam, MA), CPT1B (ABclonal, MA), c-Myc, p27 and cyclin D1 (Cell Signaling Technology, MA), cyclin A1, and cyclin E1 (Sangon Biotechnology, Shanghai, China), followed by incubation with secondary anti-rabbit or anti-mouse antibodies (Cell Signaling Technology) at room temperature. Blots were developed using an electro-chemiluminescence kit (Engreen Biosystem, Beijing, China) and a chemiluminescence imaging system (GE Healthcare, NJ). The intensity of protein bands was assayed using Quantity One software (Bio-Rad Laboratories, CA).

## 2.5 | Senescence-associated $\beta$ -galactosidase staining and colony formation assay

To detect the activity of senescence-associated  $\beta$ -galactosidase (SA- $\beta$ -gal) at pH 6.0, the cells were washed with PBS, fixed with glutaraldehyde for 15 min, and then washed again after transfection for 72 hr. Then, the cells were stained for 12–16 hr by using the Senescence  $\beta$ -Galactosidase Staining Kit (Beyotime Biotechnology, Shanghai, China). Photographs were taken using an inverted fluorescence microscope (Olympus, Tokyo, Japan) at 400 $\times$  magnification.

Colony formation assays were done by seeding 5,000, 2,500 or 1,250 cells per well in 6-well plates and allowing cells to form colonies for 2 weeks. The cells were fixed with 4% formaldehyde and stained with Diff-Quik (Propbs Biotechnology, Beijing, China) or crystal violet (Beyotime Biotechnology).

## 2.6 | Bromodeoxyuridine incorporation assay and cell cycle analysis

Bromodeoxyuridine (BrdU) incorporation was examined by use of a Cell Proliferation ELISA, BrdU (colorimetric) kit (Roche Applied Science, CA). The cells were transfected for 48 hr, labeled with BrdU for another 24 hr, and then fixed in situ and incubated with an anti-BrdU antibody. The absorbance was detected at a wavelength of 370 nm with a reference wavelength of 492 nm.

For cell cycle analysis, the cells were fixed with 70% cold ethanol at 4°C overnight and then stained with propidium iodide according to the manufacturer's protocol using the Cell Cycle and Apoptosis Analysis Kit (Beyotime Biotechnology). The cell cycle was measured by flow cytometry (Beckman Coulter, CA) at 488 nm wavelength and the data were processed with FlowJo Version 7.6.1 (Treestar, OR).

## 2.7 | Lipidomics analysis

Lipidomics analysis was performed according to our previously reported methods (Zhang et al., 2017). In short, the cells were lysed by two cycles of freezing in liquid nitrogen and thawing at 37°C for 10 min, followed by sonication for 30 s on ice. For lipid extraction, 1.2 ml of chilled methanol/methyl-tert-butyl ether/H<sub>2</sub>O (4:5:5, v/v/v) was added into the cell suspension. After being vortexed for 2 min and kept on ice for 10 min, the mixture was centrifuged at 1,000 rpm for 5 min at 4°C to precipitate protein and particulates. The upper supernatant was transferred into a clean tube and dried under vacuum. The samples

were resuspended in isopropanol/methanol (1:1, v/v) for further ultra-high-performance liquid chromatography coupled with electrospray ionization high-resolution mass spectrometry (UHPLC-ESI-MS) analysis using an Ultimate 3000 HPLC system (Dionex Corporation, CA) interfaced with a Q Exactive™ benchtop Orbitrap high-resolution mass spectrometer (Thermo Fisher Scientific). The chromatographic separation and MS analysis were performed according to the conditions we reported previously (Zhang et al., 2017).

The mass spectra data were processed using Xcalibur software version 2.2 (Thermo Fisher Scientific). LipidSearch software (Thermo Fisher Scientific) was applied to automatically identify lipid molecular and evaluate extractability by comparing peak abundances based on accurate precursor  $m/z$  and MS/MS raw data, referring a large-scale database. The multivariate data matrix containing aligned peak areas with matched  $m/z$  and retention times was further exported into SIMCA-P 13.0 software (Umetrics, NJ). Unsupervised principal components analysis (PCA) was constructed to analyze the differences in lipidomic signatures.

## 2.8 | Oil Red O and Nile Red staining assays

The intracellular lipid content was assessed by Oil Red O and Nile Red staining assays. After 72 hr of siRNA transfection, the cells were washed with PBS twice and then fixed in 4% paraformaldehyde for 30 min at room temperature. For Oil Red O staining, a 1% stock solution of Oil Red O (Sangon Biotechnology) was prepared in isopropanol. The cells were stained with a newly prepared work solution of Oil Red O (stock solution/H<sub>2</sub>O, 3:2, v/v) in the dark for 15 min. The images were taken using an inverted fluorescence microscope (Olympus) at 400 $\times$  magnification. For Nile Red staining, a 5 mg/ml stock solution of Nile Red (Sangon Biotechnology) was prepared in dimethylsulphoxide (DMSO). The cells were stained with a newly prepared working solution of Nile Red (5  $\mu$ g/ml) in the dark for 15 min. The intensity of fluorescence was detected by a multi-functional microplate reader Flex Station 3 (Molecular Devices, CA) at an excitation wavelength of 543 nm and an emission wavelength of 598 nm.

## 2.9 | Detection of reactive oxygen species and mitochondrial membrane potential

Intracellular reactive oxygen species (ROS) accumulation was measured with an oxidation-sensitive fluorescent probe, 6-carboxy-2',7'-dichlorodihydrofluorescein diacetate (Beyotime Biotechnology), which is oxidized to a fluorescent compound 2,7-dichlorofluorescein (DCF) in the presence of ROS. DCF intensity was detected using the Flex Station 3 (Molecular Devices) at an excitation wavelength of 488 nm and an emission wavelength of 525 nm. The protein concentration for each sample was used for normalization.

The loss of mitochondrial membrane potential was determined by the mean fluorescence intensity of rhodamine 123 (RH123) (Sigma-Aldrich, MO). Samples were analyzed using the Flex Station 3 (Molecular Devices) with an excitation wavelength of 488 nm and

an emission wavelength of 525 nm. The protein concentration for each sample was used for normalization.

## 2.10 | Oxygen consumption rate measurement using Seahorse Cellular Flux assays

The oxygen consumption rate (OCR) was examined using a Seahorse XF-24 Extracellular Flux Analyzer (Seahorse Bioscience, MA) to assess mitochondrial respiration as described previously (Nie et al., 2013). Briefly,  $1 \times 10^5$  cells were seeded on a special plate overnight. The OCR was measured under basal conditions and after the addition of oligomycin (1  $\mu$ M), Carbonyl cyanide-4 (trifluoromethoxy) phenylhydrazone (FCCP, 0.25  $\mu$ M), and rotenone (0.5  $\mu$ M)/antimycin A (0.5  $\mu$ M). The OCR values were normalized by the cell number counted with a Cellometer AutoT4 (Nexcelom Bioscience, MA).

## 2.11 | Statistical analysis

All data are presented as the means  $\pm$  standard deviation. The differences between groups were assessed using a Student *t* test or the nonparametric Mann-Whitney U-test using SPSS 19.0 software (IBM Analytics, NY), and graphs were prepared using GraphPad Prism 6.0 software (GraphPad Software Incorporated, CA). Each experiment was performed at least three times independently. For lipidomic analysis, a false discovery rate (FDR) control was used to correct for multiple comparisons using the SAS PROC MULTITEST with the FDR option (SAS Institution, NC). *p* values less than 0.05 were considered statistically significant while controlling the FDR at 0.05. Significance was represented by \**p* < 0.05, \*\**p* < 0.01, \*\*\**p* < 0.001, #*p* < 0.0001 versus the siControl group.

## 3 | RESULTS

### 3.1 | Effects of CPTs knockdown on PANC-1 and MDA-MB-231 cellular proliferation and senescence

We recently reported that CPT1C plays a vital role in cancer cellular senescence and proliferation (Wang et al., 2018). Here, we assessed whether other CPT members, including CPT1A, CPT1B, and CPT2, had the same effects on cellular senescence as CPT1C. Quantitative RT-PCR and Western blot revealed significant reductions in CPT1A, CPT1B, CPT1C, and CPT2 mRNA and protein levels in PANC-1 (Supporting Information Figure S1A and B) and MDA-MB-231 cells (Supporting Information Figure S1C and D) after transfection with siRNA CPTs. Cellular senescence was monitored by SA- $\beta$ -gal staining and the senescence-associated secretory factor (SASP) interleukin-8 (*IL-8*) mRNA level after transfection of siRNA against CPTs for 72 hr. Strong positive staining for senescence-associated galactosidase was observed in the siRNA CPT1C group of these two cell lines, whereas the cells knocked down for other CPT genes were nearly negative for  $\beta$ -gal (Figure 1a). Additionally, the mRNA expression levels of a key SASP factor (*IL-8*) were markedly increased the most among the

siCPTs groups in PANC-1 cells (4.2-fold) and MDA-MB-231 cells (5.4-fold) by depletion of CPT1C (Figure 1b).

Next, the effects of CPTs knockdown on senescence-associated cell proliferation were compared. The CPT1C siRNA-treated group showed a significant decrease in DNA synthesis revealed by the measurement of BrdU incorporation with a percentage of 55.5% in PANC-1 cell and 19.4% in MDA-MB-231 cell. CPT1B knockdown also decreased replicating DNA to a lesser extent in both cell lines, and CPT2 knockdown reduced it by 19.9% in MDA-MB-231 cells (Figure 1c). In addition, depletions of CPT1A, CPT1C, and CPT2 in these two cell lines had weaker colony-forming capacities than the negative control, and CPT1C knockdown had the strongest impact on the inhibition of cell growth (Figure 1d). Furthermore, CPT1C-depleted PANC-1 and MDA-MB-231 cells arrested the cell cycle in G1 phase, changing this cell population from 30.0% to 58.0% and 50.3% to 56.0%, respectively. The knockdown of CPT1A, CPT1B, and CPT2 showed a proportion in the G1 phase of 46.4%, 40.9%, and 43.4% in PANC-1 cells and 42.0%, 44.5%, and 46.1% in MDA-MB-231 cells (Figure 1e,f). Taken together, these results indicated that the effect of CPT1C on senescence-like growth arrest and cell senescence was more significant than that of other CPT members.

### 3.2 | Change of lipids in PANC-1 cell after CPTs knockdown

CPTs are essential for the import of fatty acid to the mitochondria for  $\beta$ -oxidation, which contributes to adenosine triphosphate (ATP) production (Bonfont, 2004). Lipidomics analysis was carried out to investigate how lipid profiles in PANC-1 cells varied, while CPT1 isoforms and CPT2 were depleted. To identify the general trends in an unbiased way, PCA was performed to reveal differences among all groups on a multivariate basis. PCA scatter diagrams obtained from positive (Figure 2a) and negative ion mode (Figure 2b) showed a clear separation of samples between each siRNA-treated groups, in spite of no segregation between the siCPT2 and siControl group in the negative ion mode, suggesting distinct discrimination in lipid profiles. And quality controls (QCs) displayed the stability and reproducibility of the operation system.

Given the mobile phases used in separation, [M + H]<sup>+</sup>, [M + Na]<sup>+</sup>, and [M + NH<sub>4</sub>]<sup>+</sup> adduct ions were considered as precursor ions in the positive ion mode and [M - H]<sup>-</sup>, [M + HCOO]<sup>-</sup> for the negative ion mode, respectively. A large number of lipid classes were identified by LipidSearch software. Cardiolipin (CL) exerts a crucial role in mitochondrial structure and function (Paradies, Paradies, Ruggiero, & Petrosillo, 2014). As shown in Figure 2c, CL decreased to a ratio of 0.7 significantly in siRNA CPT1C-treated cells and increased to 1.3 in the siCPT2 group compared with the negative control, indicating that mitochondrial dysfunction might be induced by CPT1C knockdown. The levels of triglycerides (TG) nearly increased in low expression of CPTs, whereas the levels of phosphatidylcholines/phosphatidylethanolamines (PC/PE ratio), lysophosphatidylcholines (LPC), lysophosphatidylethanolamines (LPE), diacylglycerols (DG), phosphatidylserines (PS), and

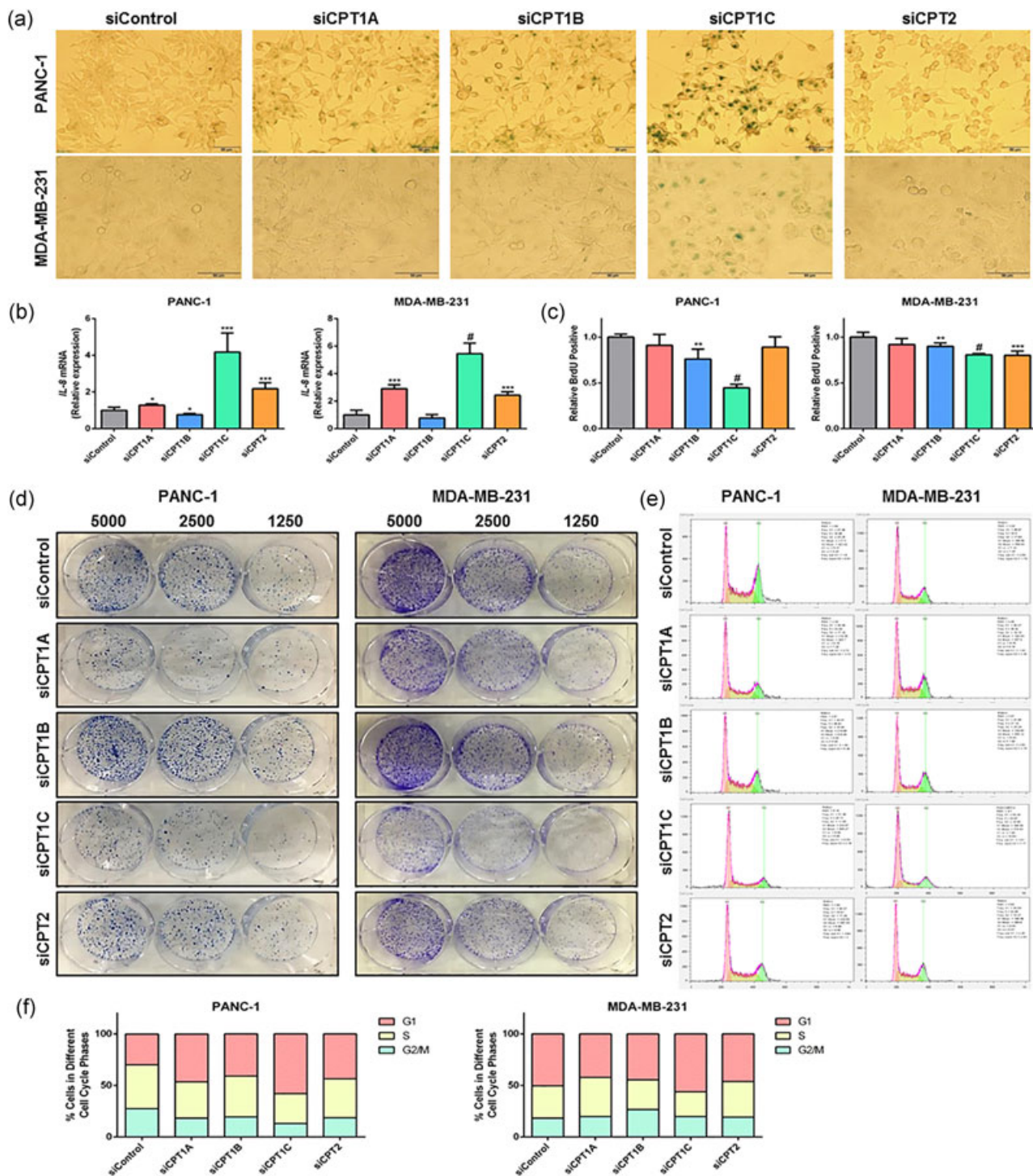


**FIGURE 1** The effects on cellular proliferation and senescence in PANC-1 and MDA-MB-231 cells after transfection with CPT1A, CPT1B, CPT1C, and CPT2 siRNA for 72 hr. (a) Representative images of SA-β-gal staining,  $n = 3$  per group. (b) Quantitative RT-PCR analysis of the key SASP factor, IL-8,  $n = 4$  per group (c) BrdU incorporation during DNA synthesis,  $n = 5$  per group. (d) Colony formation at the indicated limiting dilution. (e) Cell cycles determined by flow cytometry. (f) Quantitation of cell cycles. Data are represented as the mean  $\pm$  SD. \* $p < 0.05$ , \*\* $p < 0.01$ , \*\*\* $p < 0.001$ , # $p < 0.0001$  compared to the siControl group. BrdU: bromodeoxyuridine; CPT: carnitine palmitoyltransferase; IL-8: interleukin-8; SA-β-gal: senescence-associated β-galactosidase; SASP: senescence-associated secretory factor; SD: standard deviation; siRNA: small interfering RNA [Color figure can be viewed at wileyonlinelibrary.com]

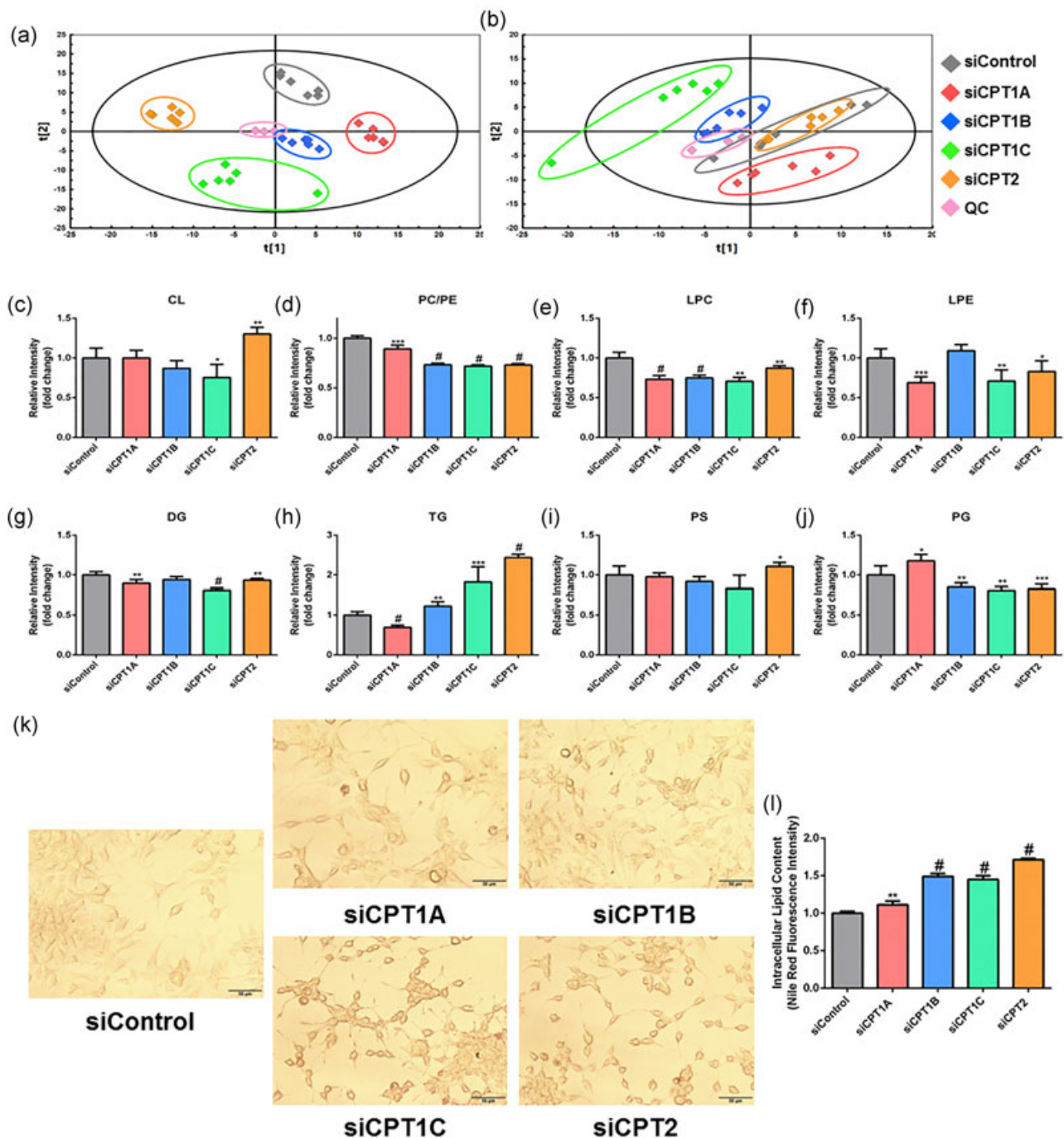


**FIGURE 2** Lipids change in PANC-1 cells when CPTs were knocked down. PCA score plots of lipidomic profiles obtained from LC-MS/MS in PANC-1 cells in positive (a) and negative (b) ion modes. Grey diamonds: negative control; red diamonds: siRNA CPT1A; blue diamonds: siRNA CPT1B; green diamonds: siRNA CPT1C; orange diamonds: siRNA CPT2; pink diamonds: quality control QCs. (c–j) The comparison of cellular lipid species content,  $n = 6$  per group. (k) Representative images of Oil Red O staining displayed at 400 $\times$  magnification. (l) Relative fluorescent intensity of intracellular lipid content by using Nile Red staining,  $n = 5$  per group. Data are represented as the mean  $\pm$  SD. \* $p < 0.05$ , \*\* $p < 0.01$ , \*\*\* $p < 0.001$ , # $p < 0.0001$  compared to the siControl group. CPT: carnitine palmitoyltransferase; PCA: principal components analysis; QCs: quality controls; SD: standard deviation; siRNA: small interfering RNA [Color figure can be viewed at [wileyonlinelibrary.com](http://wileyonlinelibrary.com)]

phosphatidylglycerols (PG) showed trends of reduction (Figure 2d–j). The detailed information about these kinds of lipid class is shown in Supporting Information Table S3.

The intracellular lipid content was further measured by the use of Oil Red O and Nile Red staining. The knockdown of CPTs

increased lipid droplets to different extents as revealed by Oil Red O staining, and this effect was more significant in the CPT1C and CPT2 deficient cells (Figure 2k). The result of Nile Red fluorescence displayed that knocking down CPT1A, CPT1B, CPT1C, and CPT2 increased intracellular lipid content

by 1.11-fold, 1.49-fold, 1.45-fold, and 1.71-fold, respectively, as shown in Figure 2l.

Overall, lipidomics based on UHPLC-ESI-MS analysis revealed different extents of the change in lipids after knockdown of CPTs, which further induced lipid accumulation.

### 3.3 | Effects of CPTs knockdown on mitochondrial function

Because lipidomics data indicated that low expression of CPTs affected the content of various lipids related to mitochondrial function such as CL, DG, TG, PS, PG, especially the knockdown of CPT1C, which markedly reduced the level of specific mitochondria lipid CL, thereby potentially impairing mitochondrial function, a series of experiments were performed to evaluate mitochondrial functions. CPT1C knockdown accumulated intracellular ROS compared with the negative control, with increased ROS level represented by the DCF intensity increase to 2.8-fold, which was higher than that in the presence of CPT1A (1.2-fold), CPT1B (1.8-fold), or CPT2 (1.4-fold) siRNA (Figure 3a). ROS can lead to free radical attack of membrane phospholipids, resulting in a loss of mitochondrial membrane potential ( $\Delta\Psi_m$ ) and matrix swelling (Li et al., 2006). As shown in Figure 3b, CPTs siRNA treatment all obviously decreased the inner mitochondrial membrane (IMM) depolarization based on the intensity of rhodamine (RH123) dye. Lower CPT1C expression caused rapid RH123 dequenching to 36.8%, which impairs the mitochondrial electrochemical gradient and permeability transition the most among all the groups.

The mitochondrial respiratory chain is the principal way to produce energy stored in ATP (Chistiakov, Shkurat, Melnichenko, Grechko, & Orekhov, 2018). OCR was then analyzed, which is an indicator of mitochondrial respiration (Figure 3c). Basal OCR, a measure of oxidative phosphorylation (OXPHOS), was markedly decreased from  $73.3 \pm 5.0$  pmol  $O_2$ /min/ $10^5$  cells in the siControl group to  $49.6 \pm 9.6$  pmol  $O_2$ /min/ $10^5$  cells in the siCPT1A group,  $47.9 \pm 5.3$  pmol  $O_2$ /min/ $10^5$  cells in the siCPT1B group,  $18.1 \pm 2.0$  pmol  $O_2$ /min/ $10^5$  cells in the siCPT1C group, and  $47.7 \pm 4.5$  pmol  $O_2$ /min/ $10^5$  cells in the siCPT2 group (Figure 3d). Addition of FCCP, which collapses the proton gradient and disrupts the mitochondrial membrane potential, augmented respiration to  $128.8 \pm 9.7$  pmol  $O_2$ /min/ $10^5$  cells in control, whereas CPT1B and CPT1C knockdown caused lower maximal respiration, with OCRs of  $86.7 \pm 11.2$  and  $49.4 \pm 6.3$  pmol  $O_2$ /min/ $10^5$  cells, respectively (Figure 3e). The same trend can be seen in spare respiration capacity (Figure 3f). Furthermore, a remarkable decrease in OCR in response to oligomycin, which inhibits ATP synthase, was found upon CPTs knockdown. Lower expression of CPT1C resulted in the most dramatic reduction on ATP production from  $57.6 \pm 4.0$  pmol  $O_2$ /min/ $10^5$  cells in control to  $23.0 \pm 2.4$  pmol  $O_2$ /min/ $10^5$  cells (Figure 3g).

Consistently, we investigated five mitochondrial complexes that are involved in the electron transport chain (ETC) (Figure 3h). Quantitative RT-PCR analysis revealed that the mRNA levels of ubiquinol-cytochrome c reductase core protein I, complex III

(UQCRC1), and cytochrome c oxidase subunit 1, complex IV (MT-CO1), ATP synthase mitochondrial F1 complex alpha subunit, complex V (ATP5A), were significantly reduced in CPT1C depleted cells, with a subtle decrease of NADH dehydrogenase 1 beta subcomplex subunit 8, complex I (NDUFB8) and succinate dehydrogenase complex, subunit A, complex II (SDHA). CPT1A and CPT2 knockdown showed an increase in complex I-V to different degrees, while CPT1B knockdown almost had no significant effect on the expression of complexes despite having a slight decrease in complex I. Mitochondrial DNA (mtDNA) is easy to become a target of oxidants produced during aging. Peroxisome-proliferator-activated receptor  $\gamma$  coactivator-1 $\alpha$  (PGC-1 $\alpha$ ) activates nuclear respiratory factor 1 (NRF1), which stimulates the expression of mitochondrial transcription factor A (TFAM), involved in duplication of mtDNA (Viña et al., 2009). The knockdown of CPTs downregulated the mRNA levels of mitochondriogenic pathway related genes to different extents as a whole. After CPT1C knockdown, PGC-1 $\alpha$ , PGC-1 $\beta$ , NRF1, and TFAM mRNA levels were significantly reduced by 24.9%, 16.3%, 34.9%, and 76.0%, respectively. Similarly, cytochrome b, one of the representative mtDNA-encoded subunits (Ide et al., 2001), was decreased by 54.1%, 30.4%, 45.0%, and 48.3% in siRNA CPT1A, CPT1B, CPT1C, and CPT2 treated groups, respectively (Figure 3i). Transcriptional profiling revealed that CPT1C knockdown impaired the renewal of mitochondria to a greater extent.

To further understand what gene expression altered exactly in CPT-mediated mitochondrial dysfunction-associated cellular senescence, we evaluated the effects of CPTs knockdown on the expression levels of genes involved in the regulation of mitochondrial genes expression including mitochondrial biogenesis, OXPHOS, the tricarboxylic acid (TCA) cycle, mitochondrial dynamics, and so on (Hock & Kralli, 2009). As shown in Figure 3J, it is notable that CPT1A, CPT1B, and CPT1C knockdown markedly downregulated the mRNA level of *c-Myc* by 59.82%, 64.32%, and 72.7%, respectively, which remained unchanged when CPT2 was knocked down. Meanwhile, CPT1C knockdown also significantly decreased the mRNA levels of estrogen relative receptor  $\alpha/\beta/\gamma$  (*ERR $\alpha/\beta/\gamma$* ), GA-binding protein  $\alpha$  subunit (*GABP $\alpha$* ), cAMP response element-binding protein (*CREB*) and CDGSH iron sulfur domain 2 (*CISD2*). The mRNA expressions of *ERR $\beta$* , *GABP $\alpha$* , *CREB* decreased and Yin Yang 1 (*YY1*), *CISD1/2* increased in the siCPT1A group, while the mRNA expression of *c-Myc*, *ERR $\alpha/\beta$* , *CREB* decreased and *CISD1* increased in the siCPT1B group. The knockdown of CPT2 downregulated the mRNA levels of *ERR $\beta/\gamma$* , *GABP $\alpha$* , *CREB* and upregulated *CISD1*.

Overall, these data suggested that CPT knockdown was involved in mitochondrial function including accumulated ROS, impaired membrane potential, downregulated respiratory capacity, decreased biogenesis and affected the transcriptional levels of genes involved in various mitochondrial functions. CPT1C made the most important contribution to induce mitochondrial dysfunction, which enhanced cellular senescence eventually.



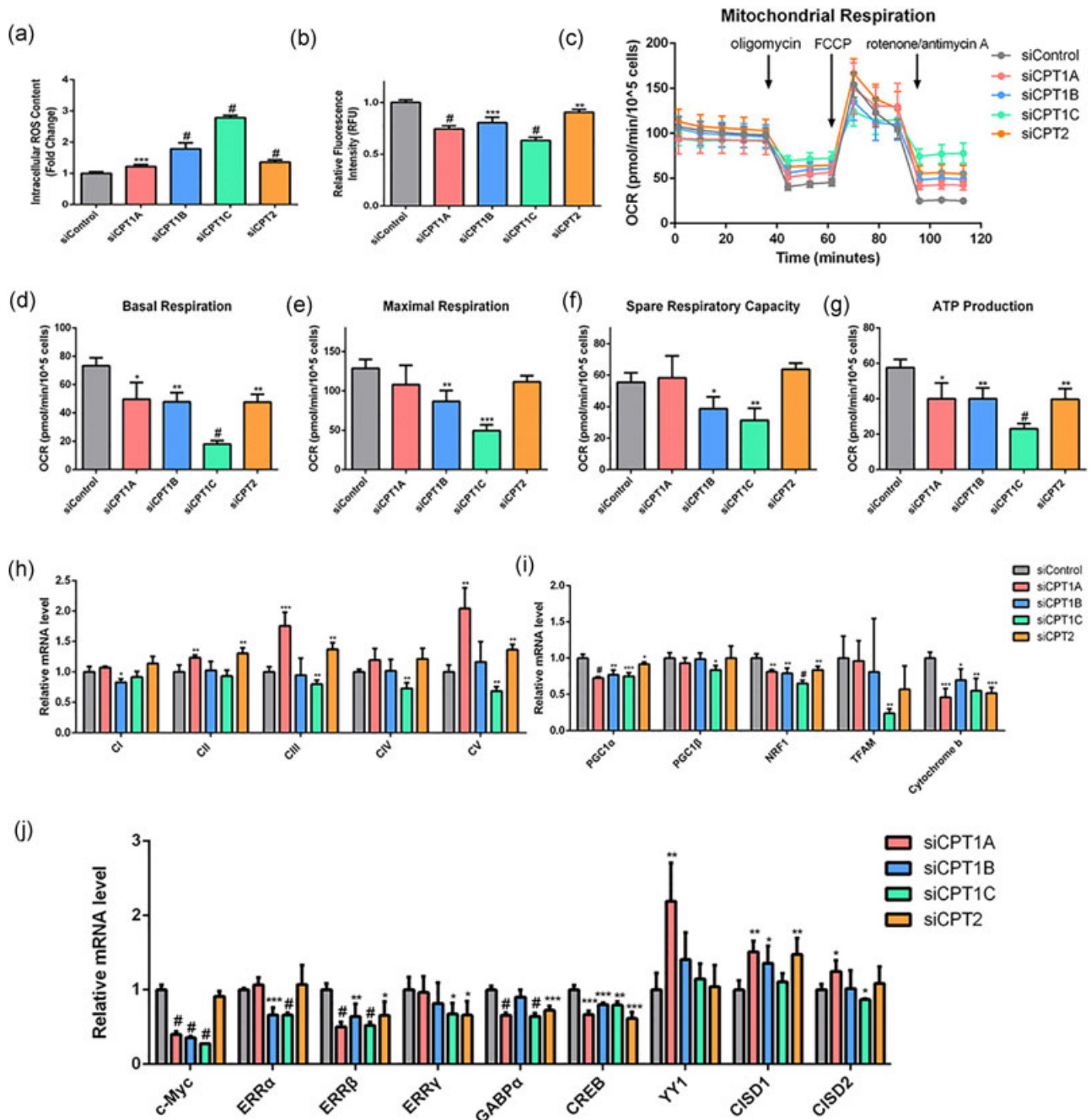


**FIGURE 3** Effects of CPTs knockdown on mitochondrial function in PANC-1 cells. Cells were transfected with siRNA CPTs for 72 hr. (a) ROS accumulation in each siRNA CPTs treated group,  $n = 5$  per group. (b) Mitochondrial transmembrane potential measured by the rh123 de-quenching method,  $n = 4$  per group. (c) Oxygen consumption rate profile plot obtained by using the Seahorse XF-24 instrument,  $n = 3$  per group. (d) Basal respiration, (e) ATP-linked respiration, (f) maximal respiration, (g) spare capacity. Basal respiration was calculated after subtraction of non-mitochondrial respiration. ATP-linked respiration was calculated following the addition of oligomycin. Maximal respiration was examined following the addition of FCCP. Spare capacity was defined as the difference between the basal and maximal respiration. (h) mRNA detection of genes encoding mitochondrial proteins involved in oxidation phosphorylation (ETC). CI: complex I (NDUFB8); CII: complex II (SDHA); CIII: complex III (UQCRC2); CIV: complex IV (MTCO1); CV: complex V (ATP5A);  $n = 4$  per group. (i) Quantitative RT-PCR detection of mitochondrial genes mRNA after siRNA knockdown of CPTs:  $n = 4$  per group. (j) mRNA levels of other genes involved in mitochondrial function:  $n = 4$  per group. Data are represented as the mean  $\pm$  SD. \* $p < 0.05$ ; \*\* $p < 0.01$ ; \*\*\* $p < 0.001$ ; # $p < 0.0001$  compared to the siControl group. CPT: carnitine palmitoyltransferase; ETC: electron transport chain; FCCP: carbonyl cyanide-4 (trifluoromethoxy) phenylhydrazone; mRNA: messenger RNA; ROS: reactive oxygen species; SD: standard deviation; siRNA: small interfering RNA [Color figure can be viewed at [wileyonlinelibrary.com](http://wileyonlinelibrary.com)]

### 3.4 | Effects of CPTs knockdown on c-Myc-controlled downstream pathway

A series of studies have documented that c-Myc is involved in cell proliferation, mitochondrial function, and cellular senescence (Wu et al., 2007). The c-Myc mRNA level was decreased dramatically in the siCPT1C group, whose protein expression was further verified. As shown in Figure 4a, CPT1C knockdown remarkably downregulated the protein expression of c-Myc by a percentage of 86.1% (Figure 4b). We further investigated the molecules associated with the signaling pathway of c-Myc. Consistent with the

observations of c-Myc expression, CPT1C knockdown dramatically activated the cell cycle inhibitor p27 to 2.3-fold (Figure 4c) and suppressed the expression of the cell cycle inducers cyclin D1, cyclin A1 and cyclin E1 to some extent compared with the siControl group (Figure 4d-f). CPT1A knockdown slightly increased c-Myc and decreased p27. Cyclin D1 elevated upon CPT1A, CPT1B and CPT2 knockdown. Hence, these results suggested that CPT1C was the only one member of the CPT family that could down-regulate c-Myc and affect its downstream pathway, subsequently inducing cell growth arrest and senescence.

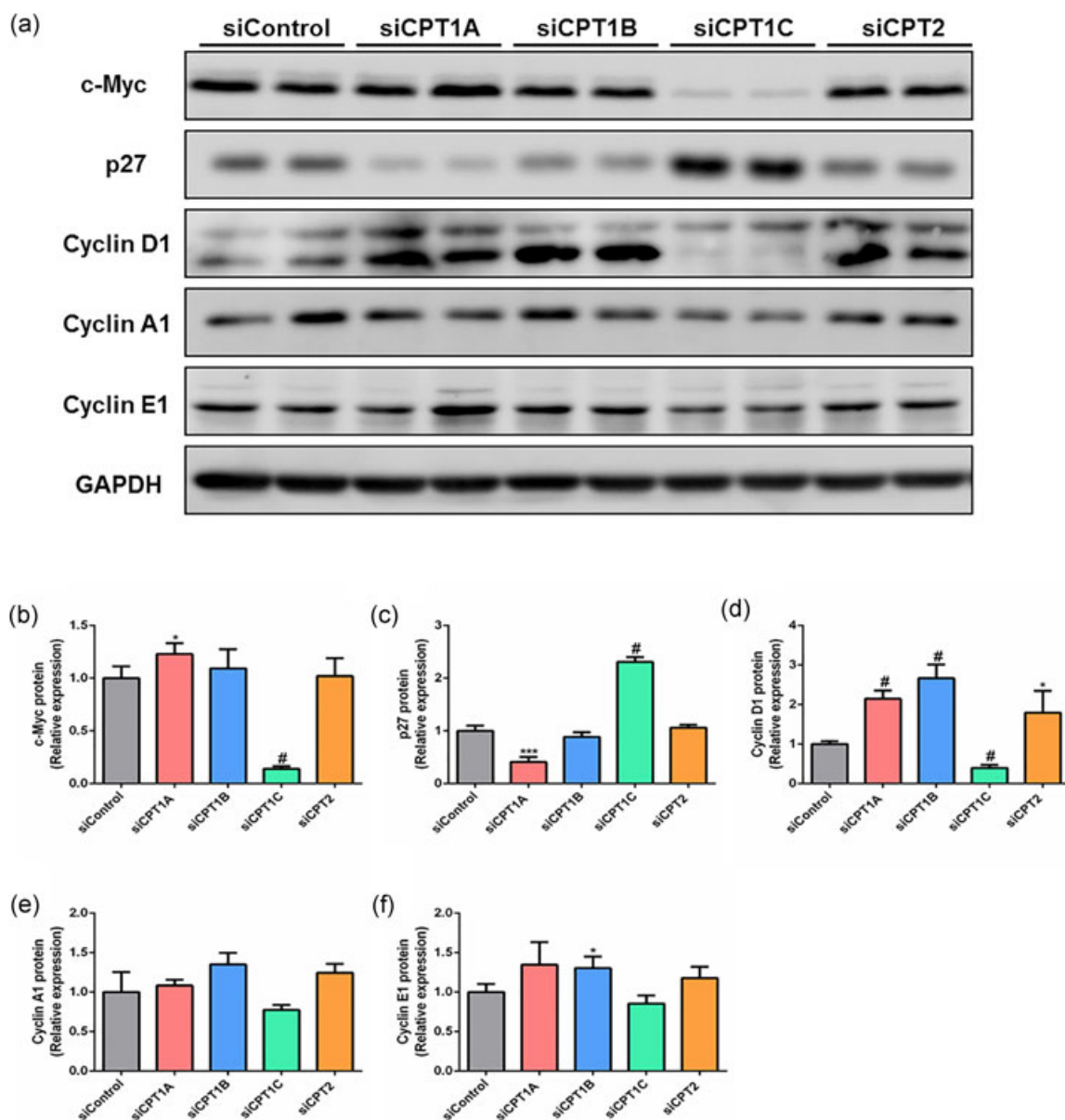


**FIGURE 4** CPTs knockdown involved in c-Myc-controlled downstream pathways. (a) Immunoblot analysis of c-Myc, p27, cyclin A/D/E in PANC-1 cell after transfection with negative control siRNA or CPTs siRNA for 72 hr. (b-f) The quantitation of immunoblots was performed by densitometric analysis. Data are expressed as the mean ± SD for at least triplicate experiments. \* $p < 0.05$ , \*\* $p < 0.01$ , \*\*\* $p < 0.001$ , # $p < 0.0001$  compared to the siControl group. CPT: carnitine palmitoyltransferase; siRNA: small interfering RNA [Color figure can be viewed at [wileyonlinelibrary.com](http://wileyonlinelibrary.com)]

## 4 | DISCUSSION

There is ample evidence that cellular senescence, a complex program that results in permanent arrest of cell division, could serve as an anticancer defense (Roninson, 2003). Our previous study demonstrated that CPT1C plays a vital role in mitochondrial dysfunction-associated cell proliferation and senescence (Wang et al., 2018). In this study, the effects of other isoforms of the CPT family, such as CPT1A, CPT1B, and CPT2, on cancer cell growth and senescence, were further investigated. As summarized in Figure 5, this study revealed that CPT1C knockdown exhibited the strongest impact on cell growth arrest and senescence, lipid change and accumulation, and mitochondrial dysfunction among all members of the CPT family. In addition, only knocking down CPT1C could downregulate the protein expression of c-Myc, cyclin D1 and upregulate the cell cycle inhibitor p27 significantly, which contributes to the potential molecular mechanism of CPT1C knockdown-induced cellular senescence. These findings further support that CPT1C may represent a new therapeutic strategy for cancer treatment through the induction of tumor senescence.

The traditional view is that the metabolic phenotype of cancer cells is featured as a preferential dependence on glycolysis (Ganapathy-Kanniappan & Geschwind, 2013). Nevertheless, growing evidence has displayed that both lipogenic and lipolytic pathways are required for carcinogenesis and tumor cell proliferation and survival. Some types of tumor cells adapt to metabolic stress like hypoxia and oncogene activation by consuming fatty acids (Kamphorst et al., 2013; Zaidi et al., 2013). Given that CPTs facilitate the entry of fatty acids into the mitochondrial matrix, which plays a crucial role in  $\beta$ -oxidation for energy production, CPTs have become potential therapeutic targets in cancer. Several studies have demonstrated that etomoxir is capable of inducing an antiproliferative effect by inhibiting CPT1A and B (Samudio et al., 2010). Moreover, treatment

with ST1326, a selective CPT1A inhibitor, showed a powerful cytotoxic activity and induced a significant delay or escape in the onset of lymphomas by blocking FAO, while treatment with AZD1480, an effective STAT3 inhibitor, downregulated CPT1B expression to inhibit FAO, resulting in suppression of breast cancer stem cell proliferation and improved chemoresistance (Pacilli et al., 2013; Wang et al., 2017). Consistent with the notion that aberrant CPT1C expression occurs in a broad array of tumor types such as neuroblastoma, liver and breast cancer, Zaugg et al. revealed that CPT1C promotes cell survival and tumor growth under conditions of glucose deprivation or hypoxia (Reilly & Mak, 2012; Zaugg et al., 2011). The loss of CPT2 incapacitates mitochondrial oxidation of LCFAs causing deleterious cardiac hypertrophic remodeling (Pereyra et al., 2017). The current results are in accord with these reports and further support the importance of CPTs in tumorigenesis. CPTs knockdown via RNA interference caused growth suppression and senescence to different degrees in PANC-1 cells, in which CPT1C played a more pivotal role from a comprehensive angle, as evidenced by lower cell proliferative and colony formative abilities, cell cycle arrest, elevated SA- $\beta$ -gal activity, and induction of SASP. A similar phenotype was also observed in MDA-MB-231 cells.

Given the close relationship between the CPT system and fatty acid transportation and oxidation, we further performed lipidomics analysis to explore a detailed and systemic lipid composition. Broad differences in lipid profiles in PANC-1 cells were observed after CPT knocking down, as revealed by PCA. It has been reported that lipid-related alterations are tightly associated with senescence. What is notable is that knocking down CPT1C markedly decreased the content of CL, indicating that mitochondrial function may be damaged. CL is a kind of unique phospholipid that is specifically localized at the IMM, suggesting its important role in mitochondrial bioenergetics processes. During aging, CL is easy to be a target of ROS. CL oxidation or depletion is linked to lower activity of the ETC

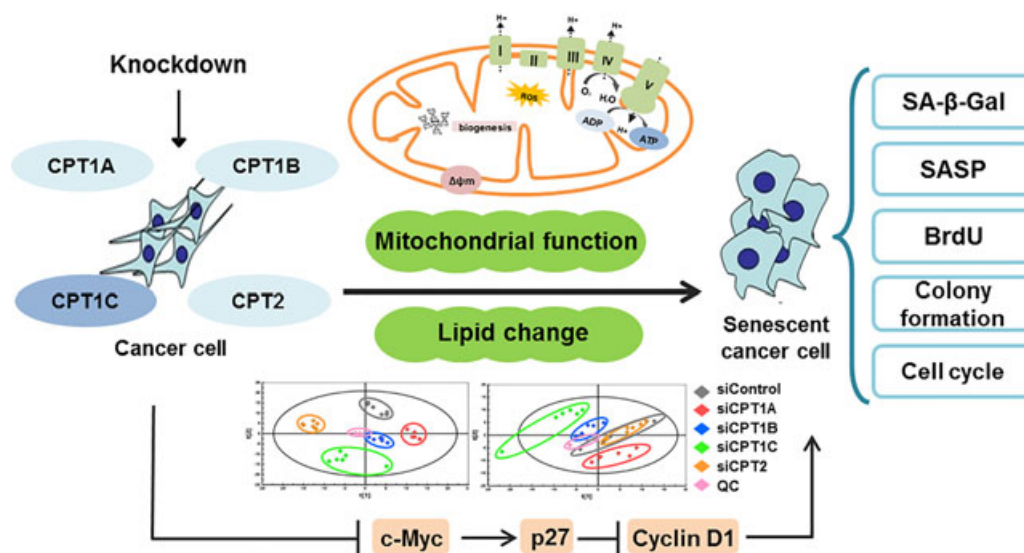


**FIGURE 5** Summary of CPTs knockdown on lipid change, mitochondrial function, cell proliferation and senescence. CPT: carnitine palmitoyltransferase [Color figure can be viewed at [wileyonlinelibrary.com](http://wileyonlinelibrary.com)]

complexes that are involved in OXPHOS and as ADP/ATP carriers, causing disruption of the mitochondrial IMM potential and abnormal mitochondrial morphology (Paradies et al., 2014). PG is required for CL synthesis. It is also crucial for mitochondrial respiratory chain activity (Mårtensson, Doan, & Becker, 2017). As main phospholipid components of this membrane, the PC/PE ratio implies membrane fluidity, which is an important parameter that affects a variety of membrane functions including signal transduction, vesicle trafficking, and transmembrane transport permeability (Fajardo, McMeekin, & LeBlanc, 2011). The results showed that siRNA CPTs transfection decreased the PC/PE ratio, indicating a reduction in membrane fluidity and, subsequently, resulting in a more rigid membrane structure. LPC and LPE also decreased upon depletion of CPTs, which was consistent with the observation of decrease in mouse brain during normal aging (Smidak, Kofeler, Hoeger, & Lubec, 2017). The lipid compositions such as DG, PE, PS, and cholesterol are required for mitochondrial morphodynamics to create a negative membrane curvature. Reductions in the content of these lipids are inclined to cause enlarged and fragmented mitochondria that are related to aging (Furt & Moreau, 2009). In the aged skeletal muscle mitochondria, DG favors the production of TG, which is critical for energy storage and maintenance of membrane composition. Nevertheless, accumulation of TG has been found in aging, obesity, and type II diabetes (Pollard, Ortori, Stöger, Barrett, & Chakrabarti, 2017; Tirosh et al., 2008). In the current study, a decrease in the level of DG and an increase of TG species were observed in the group with CPT1C knockdown, points known to be associated with cellular senescence. TG apparently enhanced more than 2-fold upon CPT2 knockdown. Consistently, the results of Oil Red O and Nile Red, which can stain neutral TGs also showed that TG accumulated in CPTs deficient cells. In agreement, liver TG content was increased in *Cpt1c* KO mice fed on high-fat diet, while CPT2 deficiency is the main factor of inherited disorder of lipid metabolism characterized lipid storage myopathy (Bonfont, 2004; Corti et al., 2008; Gao et al., 2009).

Because CPT is localized to the mitochondrial membrane and knockdown of CPTs could affect mitochondrial function-related lipids such as CL, DG, TG, PS, PG, especially CL, which was significantly reduced by knocking down CPT1C, the role of CPT1C in mitochondrial function was further compared with other CPT isoforms. Evidence shows that mitochondrial dysfunction may play a causal role during the aging process (Gallage & Gil, 2016). The mitochondrial "vicious cycle" theory of aging proposed that the accumulation of mtDNA mutations and deletions may result in impaired respiratory function and enhanced ROS production, which consequently lead to aging (Hiona & Leeuwenburgh, 2008). The present data demonstrated that CPT knockdown elevated ROS levels and disrupted the mitochondrial membrane potential and damaged mitochondriogenesis pathways to different extents, which is relevant to the impairment of mtDNA and subsequently leads to senescence. There is a report that suggests that CPT1C depletion reduced ATP production and altered fatty acids homeostasis in tumors (Zaugg et al., 2011). Consistently, we also manifested that ATP synthesis levels dramatically declined in the cells that were deficient in CPT1C as evidenced by a cellular energy

metabolism assay. The assessment of mitochondrial respiration also revealed more obvious reductions in basal, maximal respiration and spare respiratory capacity via CPT1C knockdown compared with other isoforms, in conformity with the lower mRNA expression of ETC complexes, indicating that impaired mitochondrial respiration in cells makes them unable to respond to energetic demands. A broad set of transcription factors regulate nuclear genes encoding mitochondrial proteins that control mitochondrial function. c-Myc, CREB, YY1 affect mitochondrial biogenesis via activating PGC-1 expression (Cunningham et al., 2007; Makela et al., 2016; Zhang et al., 2007). ERRs, GABP $\alpha$  are involved in the regulation of a wide set of mitochondrial genes including components of OXPHOS, mitochondrial import, the TCA cycle and so on (Giguere, 2008; Scarpulla, 2008). CISD1 and CISD2 contribute to mitochondrial homeostasis, while CISD1 overexpression can promote lipid intake and storage (Kusminski et al., 2012; Sohn et al., 2013). Our result showed that CPT1C knockdown decreased the transcriptional level of most of these genes, further suggesting that mitochondrial dysfunction was induced. Taken together, knocking down of CPT1C triggers more severe abnormalities of energy metabolism and collapse of mitochondrial function in PANC-1 cells.

The underlying molecular mechanisms involved in cellular senescence induced by CPT1C still remain unclear. c-Myc is a proto-oncogene that is involved in various biological processes, including cellular proliferation, differentiation, apoptosis, protein biosynthesis and so on (Dang et al., 2006). It is estimated that c-Myc binds and regulates up to 15% of all cellular transcriptional activity. The overexpression of c-Myc is associated with tumorigenesis, while the suppression of c-Myc has been shown to induce cellular senescence in diverse tumor types (Wu et al., 2007). Indeed, our results demonstrated that knocking down of CPT1C downregulated the mRNA level of c-Myc to a larger extent compared with other transcriptional factors, whose protein expression was further verified to be decreased remarkably, while no apparent change was observed in CPT1A, CPT1B, and CPT2 siRNA treated cells. Similarly, CPT1C was also the only CPT isoform to activate p27, an inhibitor of cyclin E/CDK2, which is repressed by c-Myc. Considering that the activation of c-Myc results in the activation of cyclin/CDK complexes, contributing to an important activity of c-Myc regulating cell proliferation that stimulates the G1-S transition (Luscher, 2001), our data agreed with this view. The sudden loss of c-Myc and activation of p27 in the cells deficient in CPT1C caused a distinct reduction in cyclin D1 and a slight decrease in cyclin A1 and cyclin E1 protein levels, resulting in cell cycle arrest in the G1 phase as revealed by flow cytometry. Therefore, CPT1C depletion induced cellular senescence by inhibiting the driving activities of c-Myc in cell proliferation and cell cycle progression.

In conclusion, this study elucidated that CPT1C is a key regulator of mitochondria-associated senescence in the comparison with other CPT isoforms (CPT1A, CPT1B, and CPT2). However, additional studies should be carried out to provide more information about the molecular mechanisms of CPT1C-induced senescence. In this scenario, CPT1C inhibition may hold promise as a therapeutic strategy for cancer treatment through induction of tumor senescence.

## ACKNOWLEDGMENTS

The authors are grateful to Dr. Jun Du from Sun Yat-sen University for generously providing MDA-MB-231 cell line.

This study was supported by the National Natural Science Foundation of China (Grants: 81522047, 81573489, 81320108027), the National Key Research and Development Program (Grant: 2017YFE0109900, 2017YFC0909303), the 111 project (Grant: B16047), the Key Laboratory Foundation of Guangdong Province (Grant: 2017B030314030), and the Natural Science Foundation of Guangdong (Grant: 2017A030311018, 2015A030313124).

## CONFLICT OF INTEREST

The authors declare that they have no conflict of interests.

## ORCID

Huichang Bi  <http://orcid.org/0000-0001-7094-2296>

## REFERENCES

- Bonnefont, J. (2004). Carnitine palmitoyltransferases 1 and 2: Biochemical, molecular and medical aspects. *Molecular Aspects of Medicine*, 25(5-6), 495-520.
- Bonnefont, J. P., Demaugre, F., Prip-Buus, C., Saudubray, J. M., Brivet, M., Abadi, N., & Thuillier, L. (1999). Carnitine palmitoyltransferase deficiencies. *Molecular Genetics and Metabolism*, 68(4), 424-440.
- Britton, C. H., Schultz, R. A., Zhang, B., Esser, V., Foster, D. W., & McGarry, J. D. (1995). Human liver mitochondrial carnitine palmitoyltransferase I: Characterization of its cDNA and chromosomal localization and partial analysis of the gene. *Proceedings of the National Academy of Sciences of the United States of America*, 92(6), 1984-1988.
- Campisi, J. (2005). Cancer: Suppressing cancer: The importance of being senescent. *Science*, 309(5736), 886-887.
- Campisi, J., & D'Adda, D. F. F. (2007). Cellular senescence: When bad things happen to good cells. *Nature Reviews Molecular Cell Biology*, 8(9), 729-740.
- Carrasco, P., Sahún, I., McDonald, J., Ramirez, S., Jacas, J., Gratacós, E., ... Casals, N. (2012). Ceramide levels regulated by carnitine palmitoyltransferase 1C control dendritic spine maturation and cognition. *Journal of Biological Chemistry*, 287(25), 21224-21232.
- Chistiakov, D. A., Shkurat, T. P., Melnichenko, A. A., Grechko, A. V., & Orekhov, A. N. (2018). The role of mitochondrial dysfunction in cardiovascular disease: A brief review. *Annals of Medicine*, 50(2), 121-127.
- Cingoz, S., Agilkaya, S., Oztura, I., Eroglu, S., Karadeniz, D., Evlice, A., ... Baklan, B. (2014). Identification of the variations in the CPT1B and CHKB genes along with the HLA-DQB1\*06:02 allele in Turkish narcolepsy patients and healthy persons. *Genetic Testing and Molecular Biomarkers*, 18(4), 261-268.
- Corti, S., Bordon, A., Ronchi, D., Musumeci, O., Aguenouz, M., Toscano, A., ... Comi, G. P. (2008). Clinical features and new molecular findings in carnitine palmitoyltransferase II (CPT II) deficiency. *Journal of the Neurological Sciences*, 266(1-2), 97-103.
- Cunningham, J. T., Rodgers, J. T., Arlow, D. H., Vazquez, F., Mootha, V. K., & Puigserver, P. (2007). mTOR controls mitochondrial oxidative function through a YY1-PGC-1alpha transcriptional complex. *Nature*, 450(7170), 736-740.
- Dang, C. V., O'Donnell, K. A., Zeller, K. I., Nguyen, T., Osthus, R. C., & Li, F. (2006). The c-Myc target gene network. *Seminars in Cancer Biology*, 16(4), 253-264.
- Demaugre, F., Bonnefont, J. P., Colonna, M., Cepanec, C., Leroux, J. P., & Saudubray, J. M. (1991). Infantile form of carnitine palmitoyltransferase II deficiency with hepatomuscular symptoms and sudden death. Physio-pathological approach to carnitine palmitoyltransferase II deficiencies. *Journal of Clinical Investigation*, 87(3), 859-864.
- Eddy, S. F., Morin, P., & Storey, K. B. (2006). Differential expression of selected mitochondrial genes in hibernating little brown bats, *Myotis lucifugus*. *Journal of Experimental Zoology Part A: Comparative Experimental Biology*, 305A(8), 620-630.
- Fajardo, V. A., McMeekin, L., & LeBlanc, P. J. (2011). Influence of phospholipid species on membrane fluidity: A meta-analysis for a novel phospholipid fluidity index. *The Journal of Membrane Biology*, 244(2), 97-103.
- Furt, F., & Moreau, P. (2009). Importance of lipid metabolism for intracellular and mitochondrial membrane fusion/fission processes. *The International Journal of Biochemistry & Cell Biology*, 41(10), 1828-1836.
- Gallage, S., & Gil, J. (2016). Mitochondrial dysfunction meets senescence. *Trends in Biochemical Sciences*, 41(3), 207-209.
- Ganapathy-Kanniappan, S., & Geschwind, J. F. H. (2013). Tumor glycolysis as a target for cancer therapy: Progress and prospects. *Molecular Cancer*, 12, 152.
- Gao, X. F., Chen, W., Kong, X. P., Xu, A. M., Wang, Z. G., Sweeney, G., & Wu, D. (2009). Enhanced susceptibility of Cpt1c knockout mice to glucose intolerance induced by a high-fat diet involves elevated hepatic gluconeogenesis and decreased skeletal muscle glucose uptake. *Diabetologia*, 52(5), 912-920.
- Giguère, V. (2008). Transcriptional control of energy homeostasis by the estrogen-related receptors. *Endocrine Reviews*, 29(6), 677-696.
- Hiona, A., & Leeuwenburgh, C. (2008). The role of mitochondrial DNA mutations in aging and sarcopenia: Implications for the mitochondrial vicious cycle theory of aging. *Experimental Gerontology Annual Reviews in Biogerontology*, 43(1), 24-33.
- Hock, M. B., & Kralli, A. (2009). Transcriptional control of mitochondrial biogenesis and function. *Annual Review of Physiology*, 71, 177-203.
- Ide, T., Tsutsui, H., Hayashidani, S., Kang, D., Suematsu, N., Nakamura, K., ... Takeshita, A. (2001). Mitochondrial DNA damage and dysfunction associated with oxidative stress in failing hearts after myocardial infarction. *Circulation Research*, 88(5), 529-535.
- Ka, S., Markljung, E., Ring, H., Albert, F. W., Harun-Or-Rashid, M., Wahlberg, P., ... Hallböök, F. (2013). Expression of carnitine palmitoyl-CoA transferase-1B is influenced by a cis-acting eQTL in two chicken lines selected for high and low body weight. *Physiological Genomics*, 45(9), 367-376.
- Kamphorst, J. J., Cross, J. R., Fan, J., de Stanchina, E., Mathew, R., White, E. P., ... Rabinowitz, J. D. (2013). Hypoxic and Ras-transformed cells support growth by scavenging unsaturated fatty acids from lysophospholipids. *Proceedings of the National Academy of Sciences of the United States of America*, 110(22), 8882-8887.
- Kusminski, C. M., Holland, W. L., Sun, K., Park, J., Spurgin, S. B., Lin, Y., ... Scherer, P. E. (2012). MitoNEET-driven alterations in adipocyte mitochondrial activity reveal a crucial adaptive process that preserves insulin sensitivity in obesity. *Nature Medicine*, 18(10), 1539-1549.
- Li, J., Tang, Q., Li, Y., Hu, B., Ming, Z., Fu, Q., ... Xiang, J. (2006). Role of oxidative stress in the apoptosis of hepatocellular carcinoma induced by combination of arsenic trioxide and ascorbic acid. *Acta Pharmacologica Sinica*, 27(8), 1078-1084.
- Luscher, B. (2001). Function and regulation of the transcription factors of the Myc/Max/Mad network. *Gene*, 277(1-2), 1-14.
- Makela, J., Tselikh, T. V., Kukkonen, J. P., Eriksson, O., Korhonen, L. T., & Lindholm, D. (2016). Peroxisome proliferator-activated receptor-gamma (PPARgamma) agonist is neuroprotective and stimulates

- PGC-1 $\alpha$  expression and CREB phosphorylation in human dopaminergic neurons. *Neuropharmacology*, 102, 266–275.
- Muñoz-Espín, D., & Serrano, M. (2014). Cellular senescence: From physiology to pathology. *Nature Reviews Molecular Cell Biology*, 15(7), 482–496.
- Mårtensson, C. U., Doan, K. N., & Becker, T. (2017). Effects of lipids on mitochondrial functions. *Biochimica et Biophysica Acta (BBA)—Molecular and Cell Biology of Lipids*, 1862(1), 102–113.
- Nie, X., Li, M., Lu, B., Zhang, Y., Lan, L., Chen, L., & Lu, J. (2013). Down-regulating overexpressed human Lon in cervical cancer suppresses cell proliferation and bioenergetics. *PLoS One*, 8(11), e81084.
- Orellana-Gavaldà, J. M., Herrero, L., Malandrino, M. I., Pañeda, A., Sol Rodríguez-Peña, M., Petry, H., ... Serra, D. (2011). Molecular therapy for obesity and diabetes based on a long-term increase in hepatic fatty-acid oxidation. *Hepatology*, 53(3), 821–832.
- Pacilli, A., Calienni, M., Margarucci, S., D'apolito, M., Petillo, O., Rocchi, L., ... Montanaro, L. (2013). Carnitine-acyltransferase system inhibition, cancer cell death, and prevention of myc-induced lymphomagenesis. *JNCI: Journal of the National Cancer Institute*, 105(7), 489–498.
- Paradies, G., Paradies, V., Ruggiero, F. M., & Petrosillo, G. (2014). Cardiolipin and mitochondrial function in health and disease. *Antioxidants & Redox Signaling*, 20(12), 1925–1953.
- Pereyra, A. S., Hasek, L. Y., Harris, K. L., Berman, A. G., Damen, F. W., Goergen, C. J., & Ellis, J. M. (2017). Loss of cardiac carnitine palmitoyltransferase 2 results in rapamycin-resistant, acetylation-independent hypertrophy. *Journal of Biological Chemistry*, 292(45), 18443–18456.
- Pollard, A. K., Ortori, C. A., Stöger, R., Barrett, D. A., & Chakrabarti, L. (2017). Mouse mitochondrial lipid composition is defined by age in brain and muscle. *Ageing (Albany NY)*, 9(3), 986–998.
- Price, N. T., van der Leij, F. R., Jackson, V. N., Corstorphine, C. G., Thomson, R., Sorensen, A., & Zammit, V. A. (2002). A novel brain-expressed protein related to carnitine palmitoyltransferase I. *Genomics*, 80(4), 433–442.
- Pérez-Mancera, P. A., Young, A. R. J., & Narita, M. (2014). Inside and out: The activities of senescence in cancer. *Nature Reviews Cancer*, 14(8), 547–558.
- Reilly, P. T., & Mak, T. W. (2012). Molecular pathways: Tumor cells co-opt the brain-specific metabolism gene CPT1C to promote survival. *Clinical Cancer Research*, 18(21), 5850–5855.
- Roninson, I. B. (2003). Tumor cell senescence in cancer treatment. *Cancer Research*, 63, 2705–2715.
- Samudio, I., Harmancey, R., Fiegl, M., Kantarjian, H., Konopleva, M., Korchin, B., ... Andreeff, M. (2010). Pharmacologic inhibition of fatty acid oxidation sensitizes human leukemia cells to apoptosis induction. *Journal of Clinical Investigation*, 120(1), 142–156.
- Scarpulla, R. C. (2008). Transcriptional paradigms in mammalian mitochondrial biogenesis and function. *Physiological Reviews*, 88(2), 611–638.
- Sierra, A. Y., Gratacós, E., Carrasco, P., Clotet, J., Ureña, J., Serra, D., ... Casals, N. (2008). CPT1c is localized in endoplasmic reticulum of neurons and has carnitine palmitoyltransferase activity. *Journal of Biological Chemistry*, 283(11), 6878–6885.
- Smidak, R., Kofeler, H. C., Hoeger, H., & Lubec, G. (2017). Comprehensive identification of age-related lipidome changes in rat amygdala during normal aging. *PLoS One*, 12(7), e0180675.
- Sohn, Y.-S., Tamir, S., Song, L., Michaeli, D., Matouk, I., Conlan, A. R., ... Mittler, R. (2013). NAF-1 and mitoNEET are central to human breast cancer proliferation by maintaining mitochondrial homeostasis and promoting tumor growth. *Proceedings of the National Academy of Sciences of the United States of America*, 110(36), 14676–14681.
- Stefanovic-Racic, M., Perdomo, G., Mantell, B. S., Sipula, I. J., Brown, N. F., & O'Doherty, R. M. (2008). A moderate increase in carnitine palmitoyltransferase 1a activity is sufficient to substantially reduce hepatic triglyceride levels. *American Journal of Physiology-Endocrinology and Metabolism*, 294(5), E969–E977.
- Tirosh, A., Shai, I., Bitzur, R., Kochba, I., Tekes-Manova, D., Israeli, E., ... Rudich, A. (2008). Changes in triglyceride levels over time and risk of type 2 diabetes in young men. *Diabetes Care*, 31(10), 2032–2037.
- Viña, J., Gomez-Cabrera, M. C., Borrás, C., Froio, T., Sanchis-Gomar, F., Martínez-Bello, V. E., & Pallardo, F. V. (2009). Mitochondrial biogenesis in exercise and in ageing. *Advanced Drug Delivery Reviews*, 61(14), 1369–1374.
- Wang, T., Fahrman, J. F., Lee, H., Li, Y.-J., Tripathi, S. C., Yue, C., ... Yu, H. (2017). JAK/STAT3-regulated fatty acid  $\beta$ -oxidation is critical for breast cancer stem cell self-renewal and chemoresistance. *Cell Metabolism*, 27, 1–15.
- Wang, Y., Chen, Y., Guan, L., Zhang, H., Huang, Y., Johnson, C. H., ... Bi, H. (2018). Carnitine palmitoyltransferase 1C regulates cancer cell senescence through mitochondria-associated metabolic reprogramming. *Cell Death and Differentiation*, 25(4), 733–746.
- Wolfgang, M. J., Kurama, T., Dai, Y., Suwa, A., Asaumi, M., Matsumoto, S., ... Lane, M. D. (2006). The brain-specific carnitine palmitoyltransferase-1c regulates energy homeostasis. *Proceedings of the National Academy of Sciences of the United States of America*, 103(19), 7282–7287.
- Wolfgang, M. J., & Lane, M. D. (2011). Hypothalamic malonyl-CoA and CPT1c in the treatment of obesity. *FEBS Journal*, 278(4), 552–558.
- Wu, C. H., van Riggelen, J., Yetil, A., Fan, A. C., Bachireddy, P., & Felsher, D. W. (2007). Cellular senescence is an important mechanism of tumor regression upon c-Myc inactivation. *Proceedings of the National Academy of Sciences of the United States of America*, 104(32), 13028–13033.
- Yamazaki, N., Shinohara, Y., Shima, A., Yamanaka, Y., & Terada, H. (1996). Isolation and characterization of cDNA and genomic clones encoding human muscle type carnitine palmitoyltransferase I. *Biochimica et Biophysica Acta (BBA)—Gene Structure and Expression*, 1307(2), 157–161.
- Zaidi, N., Lupien, L., Kuemmerle, N. B., Kinlaw, W. B., Swinnen, J. V., & Smans, K. (2013). Lipogenesis and lipolysis: The pathways exploited by the cancer cells to acquire fatty acids. *Progress in Lipid Research*, 52(4), 585–589.
- Zaug, K., Yao, Y., Reilly, P. T., Kannan, K., Kiarash, R., Mason, J., ... Mak, T. W. (2011). Carnitine palmitoyltransferase 1C promotes cell survival and tumor growth under conditions of metabolic stress. *Genes and Development*, 25(10), 1041–1051.
- Zhang, H., Gao, P., Fukuda, R., Kumar, G., Krishnamachary, B., Zeller, K. I., ... Semenza, G. L. (2007). HIF-1 inhibits mitochondrial biogenesis and cellular respiration in VHL-deficient renal cell carcinoma by repression of C-MYC activity. *Cancer Cell*, 11(5), 407–420.
- Zhang, H., Gao, Y., Sun, J., Fan, S., Yao, X., Ran, X., ... Bi, H. (2017). Optimization of lipid extraction and analytical protocols for UHPLC-ESI-HRMS-based lipidomic analysis of adherent mammalian cancer cells. *Analytical and Bioanalytical Chemistry*, 409(22), 5349–5358.

## SUPPORTING INFORMATION

Additional supporting information may be found online in the Supporting Information section at the end of the article.

**How to cite this article:** Guan L, Chen Y, Wang Y, et al. Effects of carnitine palmitoyltransferases on cancer cellular senescence. *J Cell Physiol*. 2018;234:1707–1719. <https://doi.org/10.1002/jcp.27042>